BIOCHEMISTRY
including biophysical chemistry & molecular biology

Article

pubs.acs.org/biochemistry

X-ray Structure and Nuclear Magnetic Resonance Analysis of the Interaction Sites of the Ga-Substituted Cyanobacterial Ferredoxin

Risa Mutoh,[†,∥] Norifumi Muraki,[†,⊥] Kanako Shinmura,[†] Hisako Kubota-Kawai,[†,∥] Young-Ho Lee,[†] Marc M. Nowaczyk,[‡] Matthias Rögner,[‡] Toshiharu Hase,[†] Takahisa Ikegami,[∥,§] and Genji Kurisu*[,†,∥]

[†]Institute for Protein Research, Osaka University, 3-2 Yamadaoka, Suita, Osaka 565-0871, Japan

[‡]Plant Biochemistry, Faculty of Biology and Biotechnology, Ruhr University Bochum, 44780 Bochum, Germany

[§]Department of Medical Life Science, Yokohama City University, 1-7-29 Suehiro-cho, Tsurumi-ku, Yokohama 230-0045, Japan

[∥]Core Research for Evolutional Science and Technology (CREST), Japan Science and Technology Agency (JST), Saitama 332-0012, Japan

Supporting Information

ABSTRACT: In chloroplasts, ferredoxin (Fd) is reduced by Photosystem I (PSI) and oxidized by Fd-NADP$^+$ reductase (FNR) that is involved in NADP$^+$ reduction. To understand the structural basis for the dynamics and efficiency of the electron transfer reaction via Fd, we complementary used X-ray crystallography and nuclear magnetic resonance (NMR) spectroscopy. In the NMR analysis of the formed electron transfer complex with Fd, the paramagnetic effect of the [2Fe-2S] cluster of Fd prevented us from detecting the NMR signals around the cluster. To solve this problem, the paramagnetic iron−sulfur cluster was replaced with a diamagnetic metal cluster. We determined the crystal structure of the Ga-substituted Fd (GaFd) from *Synechocystis* sp. PCC6803 at 1.62 Å resolution and verified its functional complementation using affinity chromatography. NMR analysis of the interaction sites on GaFd with PSI (molecular mass of ∼1 MDa) and FNR from *Thermosynechococcus elongatus* was achieved with high-field NMR spectroscopy. With reference to the interaction sites with FNR of *Anabaena* sp. PCC 7119 from the published crystal data, the interaction sites of Fd with FNR and PSI in solution can be classified into two types: (1) the core hydrophobic residues in the proximity of the metal center and (2) the hydrophilic residues surrounding the core. The former sites are shared in the Fd:FNR and Fd:PSI complex, while the latter ones are target-specific and not conserved on the residual level.

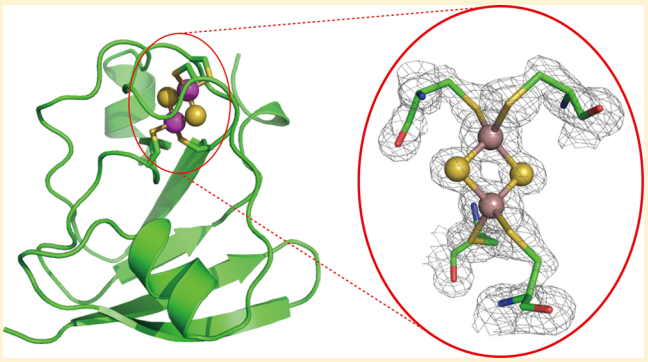

Plant-type ferredoxin (Fd) is an electron transfer protein with a [2Fe-2S] cluster, carrying one electron to Fd-dependent enzymes that are important for assimilatory and regulatory reactions in photosynthetic organisms.[1] In chloroplasts, Fd is reduced by Photosystem I (PSI) and oxidized by Fd-NADP$^+$ reductase (FNR) involved in NADP$^+$ reduction. Electron transfer from PSI to Fd is realized by a protein−protein complex that is suitable for an efficient redox reaction. After the intermolecular electron transfer, this complex dissociates quickly, which is the reason for the high rate of turnover of the light-driven photosynthetic electron transport chain. Besides Fd and PSI, this transient protein−protein interaction is also realized for other Fd-dependent enzymes such as FNR. Although Fd-dependent enzymes including PSI vary in molecular size and prosthetic groups, they all specifically recognize Fd and form a fully functional complex even without any common Fd-binding motif or fold.

To understand the structural basis for the dynamics and efficiency of the electron transfer reaction around Fd, we studied such electron transfer complexes both by crystal structure analysis of each protein and by biochemical assays characterizing mutational effects[2] and cross-linking experiments.[3] Crystal structures of plant-type Fds,[4−9] PSI, and various Fd-dependent enzymes, such as FNR,[10−14] Fd-thioredoxin reductase (FTR),[15] nitrite reductase (NiR),[16] and Fd-dependent glutamate synthase,[9] have already been reported. Also, X-ray crystallography has been used to determine the three-dimentional structure of the protein−protein complex showing a possible mode of interaction.[15,17,18] On the other hand, it is difficult to crystallize the transient electron transfer complex of target proteins. Complementary, nuclear magnetic resonance (NMR) spectroscopy has been used to analyze the interaction sites of Fd with various target proteins in solution. Instead of crystallization of the complex, NMR analysis requires the uniform labeling with isotopes such as ^{15}N for a chemical shift perturbation, permitting the analysis of Fd interaction sites

Received: June 3, 2015
Revised: September 6, 2015
Published: September 8, 2015

DOI: 10.1021/acs.biochem.5b00601
Biochemistry 2015, 54, 6052−6061

for Fd-dependent enzymes, such as Fd:FNR,[17,19] Fd:FTR,[20] Fd:NiR,[7] and Fd:sulfite reductase,[21] in solution by NMR spectroscopy. To understand the dynamic formation of a complex between Fd and Fd-dependent enzymes, a multidisciplinary approach for the structural characterization of the complex is necessary.

During NMR analysis of formation of the Fd complex, the fast nuclear relaxation of the nuclear spins caused by the [2Fe-2S] cluster prevents us from detecting the NMR signals from the residues around the cluster. To solve this problem, replacement of the paramagnetic iron−sulfur cluster with a diamagnetic metal or metal cluster has been proposed.[22] Ga(III) was frequently used to form a complex analogous to that of Fe(III) because of the similarity of the ionic radii and coordination chemistry of the two ions. However, there have been conflicting characterization studies of the metal centers of plant-type Ga-substituted Fd (GaFd) from two cyanobacteria. A reconstituted gallium−sulfur cluster in Fd of *Anabaena* sp. PCC 7120 was assigned the formula [2Ga-2S],[23] while that of *Synechocystis* sp. PCC 6803 (hereafter named *Synechocystis*) was independently assigned as [1Ga-0S],[19] a rubredoxin-like single-metal center.

Although the NMR structure of *Synechocystis* GaFd with a single Ga(III) ion has already been reported, the solution structure showed distortion in the metal-binding loop region.[19] To conclusively determine the chemical composition of a gallium−sulfur cluster from plant-type GaFd and to estimate the extent to which the reconstituted cluster resembles the native [2Fe-2S] cluster, X-ray crystallography of GaFd is essential. Here, we determined the crystal structure of GaFd from *Synechocystis* at 1.62 Å resolution and verified its functional complementation using affinity chromatography. After confirming the structural identity of *Synechocystis* GaFd, we applied the Ga substitution method to thermostable Fd from the cyanobacterium *Thermosynechococcus elongatus* because the Fd and PSI from *T. elongatus* have a substantial advantage in stability during NMR measurement. NMR analysis of the interaction sites on *T. elongatus* GaFd with PSI (mass of ∼1 MDa) has been identified by high-field NMR. In combination with the NMR data of the Fd:FNR complex from *T. elongatus*, we can show that the interaction sites of Fd with FNR and PSI are different in solution: they show flexible characteristics of the hydrophilic interactions surrounding the hydrophobic core and common interactions in the proximity of the metal center.

MATERIALS AND METHODS

Purification of Native Fd and Preparation of GaFd. A DNA fragment encoding Fd was cloned into the pET28a vector (Novagen) using the *Nco*I−*Bam*HI restriction sites. Native Fds from *Synechocystis* and *T. elongatus* and ^{15}N-labeled Fd from *T. elongatus* were all expressed in *Escherichia coli* strain BL21-(DE3) using a Luria-Bertani (LB) medium and M9 minimal medium (containing $^{15}NH_4Cl$ as the sole nitrogen source) supplemented with kanamycin (50 μg/mL). Cells were harvested by centrifugation, resuspended in 50 mM Tris-HCl buffer (pH 7.5) containing 10% (w/v) glycerol, and disrupted by sonication. The lysates were clarified by centrifugation and purified by affinity chromatography on a model DE52 anion exchanger (Whatman). After elution with 500 mM NaCl in 50 mM Tris-HCl buffer (pH 7.5), Fd samples were dialyzed at 4 °C against 1 L of 50 mM Tris-HCl buffer (pH 7.5) containing 50 mM NaCl. Dialysates were then applied to a HiTrap Q HP column (GE Healthcare), followed by a Phenyl Sepharose column (GE Healthcare) to purify the Fd samples and a Hiload 26/60 Superdex 75 column (GE Healthcare) equilibrated with 20 mM Tris-HCl buffer (pH 7.5) containing 150 mM NaCl.

The concentration of native Fd was calculated with a molar extinction coefficient (ε_{422} = 9.68 mM^{-1} cm^{-1}). *Synechocystis* GaFd and *T. elongatus* ^{15}N-labeled GaFd were prepared according to the method described in ref 20 with minor modifications. Concentrated HCl was added to 45 mg of Fd to achieve a final concentration of 1 M. The cloudy solution was centrifuged for 10 min at 17800*g*, and the white precipitate was immediately rinsed with Milli-Q water, followed by resuspension in 100 mM Tris-HCl buffer (pH 8.0). The same procedure was repeated twice to remove the Fe atoms completely. The final protein precipitate was resuspended in 100 mM Tris-HCl buffer (pH 8.0) containing 6 M guanidine hydrochloride and 10 mM dithiothreitol in the anaerobic tent. Apo-Fd was refolded at 4 °C by dilution into the refolding buffer [2 mM $GaCl_3$, 2 mM Na_2S, 2 mM dithiothreitol, and 20 mM Tris-HCl buffer (pH 8.0)]. This solution was incubated at 4 °C overnight under anaerobic conditions before application on a HiTrap-Q column (GE Healthcare), from which the protein was eluted by a gradient from 0 to 1 M NaCl in 20 mM Tris-HCl (pH 8.0). Elution profiles of the proteins have been monitored by absorbance at 280 nm, and the eluted fractions have been collected and concentrated by ultrafiltration. GaFd was then applied to a Hiload 26/60 Superdex 75 column (GE Healthcare) equilibrated with 20 mM Tris-HCl (pH 7.5) containing 150 mM NaCl. The concentration of GaFd was determined from the molar extinction coefficient (ε_{280} = 170.2 mM^{-1} cm^{-1}).

Purification of FNR_L from *Synechocystis*. In cyanobacterial cells, two forms of the FNR molecule, a full-length FNR (FNR_L) with additional phycobilisome-binding domain and a truncated FNR (FNR_S) similar in size to the plastidic FNR, function distinctively.[24−28] A full-length gene product of *petH* encoding cyanobacterial FNR consists of three functional domains: a CpcD-like domain binding phycobilisomes, an FAD-binding domain, and an $NADP^+$-binding domain. FNR_L was expressed in *E. coli* [BL21(DE3)] cells in LB medium and purified via the His tag at the N-terminus using Ni-nitrilotriacetic acid affinity chromatography. After elution with 150 mM imidazole in 50 mM Tris-HCl buffer (pH 8.0), FNR was dialyzed at 4 °C against 1 L of 20 mM Tris-HCl buffer (pH 7.5) containing 50 mM NaCl and 0.5 mM EDTA. Dialysates were then applied to a HiTrap Q HP column (GE Healthcare) to purify FNR_L, followed by application to a Hiload 16/60 Superdex 200 column (GE Healthcare) equilibrated with 20 mM sodium phosphate buffer (pH 6.8) containing 50 mM NaCl.

Purification of FNR_S and PSI from *T. elongatus*. FNR_S, corresponding to *T. elongatus* plastidic FNR without a CpcD-like domain, was expressed and purified like FNR_L of *Synechocystis* (see the section "Purification of FNR_L from *Synechocystis*"). PSI, His-tagged at the N-terminus of the PsaF subunit (on the luminal side),[29] was purified according to the purification of PSI from *Synechocystis*.[30]

Preparation of an FNR_L-Immobilized Resin and the Procedure for Affinity Chromatography. We moistened 1 mg of CNBr-activated Sepharose 4B (GE Helthcare) with 1 mM HCl and then washed the mixture with 5 mL of 1 mM HCl, followed by resuspension of 50 mg of *Synechocystis* FNR_L in 50 mM phosphate buffer (pH 6.8) containing 500 mM

DOI: 10.1021/acs.biochem.5b00601
Biochemistry 2015, 54, 6052−6061

Table 1. Crystallographic Data of Ga-Substituted Ferredoxin (GaFd) from *Synechocystis* sp. PCC 6803 and Fd from *T. elongatus*

	GaFd from *Synechocystis* sp. PCC6803		Fd from *T. elongatus*
	native	anomalous	native
X-ray source	SPring-8 BL44XU	SPring-8 BL38B1	PF BL1A
detector	MX-225HE	ADSC-Q315	Dectris PILATUS 2M-F
wavelength (Å)	0.90000	1.90000	1.1000
space group	$P6_122$	$P6_122$	$C2$
unit cell parameters			
a (Å)	31.94	31.96	56.44
b (Å)	31.94	31.96	53.31
c (Å)	320.08	320.08	32.28
α (deg)	90	90	90
β (deg)	90	90	92.38
γ (deg)	120	120	90
resolution range (Å)	40.0−1.62 (1.65−1.62)[a]	50.0−2.50 (2.59−2.50)[a]	50.0−1.50 (1.53−1.50)[a]
total no. of reflections	189967	67440	48635
no. of unique reflections	13883	4114	15300
completeness (%)	96.6 (91.1)[a]	99.5 (100)[a]	98.8 (93.6)[a]
$R_{merge}(I)$ (%)[b]	6.4 (33.3)[a]	7.9 (25.0)[a]	6.1 (29.1)[a]
I/σ	64.1 (10.2)[a]	9.0 (8.76)[a]	35.5 (3.9)[a]
	Refinement		
resolution range (Å)	27.56−1.62 (1.66−1.62)		32.25−1.50 (1.53−1.50)
R_{work}	0.198 (0.168)	–	0.172 (0.205)
R_{free}	0.219 (0.199)	–	0.193 (0.196)
mean B value (Å^2)	23.438	–	23.162
no. of non-hydrogen atoms, including dual conformers			
protein	715	–	760
metal cluster	4	–	4
water	36	–	37
rmsd from ideal values			
bond lengths (Å)	0.018	–	0.011
bond angles (deg)	1.921	–	1.841

[a]Values in parentheses are for the highest-resolution shells. [b]$R_{merge}(I) = \sum|I(k) - \langle I\rangle|/\sum I(k)$, with $I(k)$ representing the k value of an intensity measurement of a reflection, $\langle I\rangle$ the mean intensity value of that reflection, and $\sum$ the summation across all measurements.

NaCl; this mixture was gently stirred at 4 °C overnight. Resins have been washed with 50 mM Tris-HCl buffer (pH 7.5) containing 500 mM NaCl to block the remaining active sites on the resin. After equilibration of the column with 20 mM Tris-HCl buffer (pH 7.5) containing 50 mM NaCl, 10 mg of GaFd or native Fd was loaded onto the column and eluted by a linear gradient of NaCl (50 to 500 mM). Elution profiles of the proteins have been monitored at 280 nm.

Heat Denaturation Curve. Circular dichroism (CD) spectra and denaturation curves of native and Ga-substituted Fd from *Synechocystis* and *T. elongatus* have been recorded in 20 mM Tris-HCl buffer (pH 7.5) containing 150 mM NaCl. The temperature of the protein solution was gradually (1 °C min^{-1}) increased from 25 to 95 °C, while the molar ellipticity was monitored at 220 nm for *Synechocystis* and at 223 nm for *T. elongatus*, followed by determination of their thermostability (T_m).

Crystallization. Initial crystallization screening was performed at 20 °C by hanging drop vapor diffusion. The concentrations of *Synechocystis* GaFd and *T. elongatus* Fd were adjusted to 10 and 20 mg/mL, respectively. Colorless hexagonal crystals of *Synechocystis* GaFd were obtained from equal volumes of the concentrated protein and reservoir solutions [100 mM MES-KOH buffer (pH 6.0) containing 3.4 M $(NH_4)_2SO_4$ and 2% (w/v) benzamidine hydrochloride]. For data collection under cryogenic conditions, crystals were soaked in the reservoir solution containing 5% (v/v) glycerol and dipped into liquid nitrogen. Using identical settings, brownish rod-shaped crystals of *T. elongatus* Fd were obtained with a different reservoir solution [100 mM sodium citrate buffer (pH 6.5) containing 2.6 M $(NH_4)_2SO_4$, 0.2% (w/v) benzamidine hydrochloride, and 3% (w/v) 1,6-hexanediol]. Crystals were soaked in a reservoir solution containing 15% (v/v) glycerol and dipped into liquid nitrogen for cryo-protection.

X-ray Experiments and Structure Determination. Using the frozen crystal of *Synechocystis* GaFd, X-ray absorption edge scans have been performed around the K-absorption edges of Ga (λ = 1.1959 Å) and Fe (λ = 1.7433 Å), via X-ray experiments at SPring-8 (Harima, Japan). Native and anomalous data sets were measured at BL44XU using an MX-225HE CCD detector (Rayonix) and at BL38B1 using an ADSC-Q315 CCD detector (ADSC). All diffraction images from *Synechocystis* GaFd were collected at 100 K using the oscillation method. We recorded 180 frames with a 1° oscillation at a wavelength of 0.90000 Å using BL44XU and 720 frames with a 0.25° oscillation at a wavelength of 1.90000 Å using BL38B1. Two sets of diffraction images were processed and scaled in the HKL-2000 software,[31] independently (Table 1). Initial phases were determined by the molecular replacement method using the crystal structure of native Fd from *Synechocystis* [Protein Data Bank (PDB) entry 1OFF[9]] using the Molrep program of the CCP4 software package.[32] The structure of *Synechocystis* GaFd was refined by the Refmac program of CCP4, and a manual revision of the atomic model

DOI: 10.1021/acs.biochem.5b00601
Biochemistry 2015, 54, 6052−6061

was conducted with COOT.[33] For crystallographic restrained refinement, we used the stereochemical geometry of a synthetic compound, $[Et_4N]_2[Ga_2S_2(SPh)_4]$,[34] from the Cambridge Crystallographic Data Center as a reference for the [2Ga-2S] cluster. An anomalous Fourier map maximizing an anomalous difference from sulfur atoms was calculated using the anomalous data set (λ = 1.90000 Å) and the phases calculated from the refined coordinates. All diffraction images from the frozen crystal of *T. elongatus* Fd were collected at beamline BL1A of the Photon Factory (KEK, Tsukuba, Japan), using the Dectris PILATUS 2M-F detector. We recorded 180 frames with a 1° oscillation at 1.1000 Å. Diffraction images were processed and scaled in the HKL-2000 software package (Table 1). Phases were determined by the molecular replacement method using the crystal structure of *Leptolyngbya boryana* Fd (PDB entry 3B2G)[7] in Molrep. The structure of *T. elongatus* Fd was refined by Refmac and COOT. Stereochemical geometry protein models of *Synechocystis* GaFd and *T. elongatus* Fd were verified with MolProbity.[35]

NMR Measurements. In NMR measurements, we used samples derived from *T. elongatus*. $^1H-^{15}N$ heteronuclear single-quantum coherence (HSQC) spectra of [^{15}N]GaFd were recorded on a Bruker Avance III spectrometer with a ^{1}H resonance frequency of 950 MHz with a TCI cryoprobe. A mixture of 100 μM [^{15}N]GaFd and 300 μM FNR_S in 20 mM sodium phosphate buffer (pH 6.8) containing 50 mM NaCl and 10% D_2O was analyzed at 298 K, and a mixture of 30 μM [^{15}N]GaFd and 1 μM PSI in 50 mM Hepes-NaOH buffer (pH 7.8) containing 150 mM NaCl, 0.04% *n*-dodecyl β-D-maltopyranoside, and 10% D_2O was analyzed at 323 K. Weighted averages of ^{1}H and ^{15}N chemical shift changes, represented (Δ_{avr}) as $\Delta\delta^1_{HN}$ and $\Delta\delta^{15}_N$, respectively, were calculated using the formula $\Delta\delta_{avr} = [(\Delta\delta^1_{HN})^2 + (0.04\Delta\delta^{15}_N)^2]^{1/2}$.

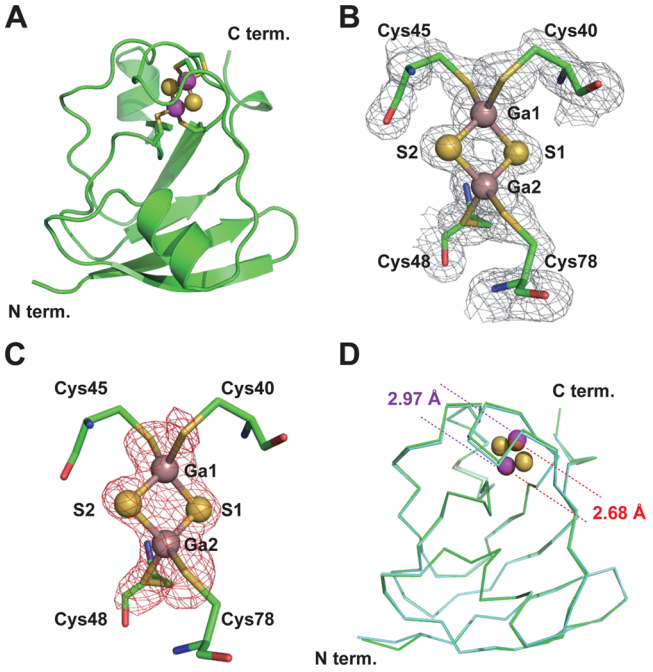

Figure 1. Core structures and comparison of *Synechocystis* Ga-substituted ferredoxin (GaFd) and native Fd. (A) Ribbon model of the *Synechocystis* GaFd structure. The [2Ga-2S] cluster is shown as a ball-and-stick model in magenta (S) and yellow (Ga). This figure was created in PyMOL.[42] (B) Final σ-weighted $2|F_o| - |F_c|$ electron density map (λ = 0.90000 Å) around the cluster. (C) Anomalous difference Fourier map (λ = 1.90000 Å) at the 3.0σ level. (D) Superimposed Cα traces of *Synechocystis* GaFd (green) and native Fd (cyan). The color codes of *Synechocystis* GaFd are identical to those in panel A. Two Fe(III) ions of the [2Fe-2S] cluster from native Fd are colored red.

RESULTS AND DISCUSSION

Determination of the Structure of *Synechocystis* GaFd. GaFd was crystallized as colorless hexagonal crystals. Crystallization conditions for native Fd and GaFd were similar in terms of buffer system and precipitant but significantly different in pH and additives.[9] Crystals of native Fd belonged to space group $P6_5$,[9] but those of GaFd belonged to space group $P6_122$ (Table 1.). The crystal structure of GaFd was determined by the molecular replacement method and refined at 1.62 Å resolution (Figure 1A). The existence of two Ga ions was confirmed by a clear-cut σ-weighted $2|F_o| - |F_c|$ electron density map (Figure 1B) and X-ray absorption fine structure (XAFS) spectra (data not shown) showing a peak near the absorption edge of Ga (λ = 1.19513 Å) and no peak around the absorption edge of Fe. The anomalous Fourier electron density map (λ = 1.90000 Å) showed that the two bridging atoms between the two Ga ions had peak heights similar to those of the ligating Sγ atoms from cysteine residues (Figure 1C). On the basis of these X-ray data, we confirmed that the composition of the cluster of GaFd was [2Ga-2S]. The final coordinates of GaFd included one Fd molecule of 96 amino acid residues and a [2Ga-2S] cluster, six molecules of benzamidine, 36 water molecules, and two sulfate ions in the asymmetrical unit. The crystallographic refinement statistics are listed in Table 1. According to MolProbity Ramachandran analysis, 100% of all residues were in the allowed regions.

Structural Comparison of Native Fd and GaFd from *Synechocystis*. Superposition of GaFd and native Fd (PDB entry 1OFF)[9] on the basis of the C_α atoms and all atoms resulted in rmsds of 0.286 and 0.549 Å, respectively (Figure 1D). While the whole structures of GaFd and native Fd were almost identical, there was only a slight difference in the terminal regions. On the other hand, the NMR structure of *Synechocystis* GaFd (PDB entry 2KAJ, model 1)[19] significantly varied, with rmsds of 1.159 Å for the C_α atoms and 2.049 Å for the whole atoms. These differences between the X-ray and NMR structures probably originated from the two cluster types, [2Ga-2S] and [1Ga-0S], and apparently were due to the minor modification of the experimental procedure for GaFd preparation. Electrostatic potentials of native Fd and GaFd were mapped on their molecular surfaces (Figure 2A). Fd is an acidic protein and has acidic patches that are important for forming a complex with Fd-dependent enzymes. The complete conservation of these acidic patches on the surface was confirmed for both molecules. A more detailed analysis of the metal clusters reveals that the replacement of Fe(III) with Ga(III) caused subtle structural changes in the cluster (Figure 1D). Most remarkably, the distance between the two metal ions is different: while the distance between the two Ga(III) ions in GaFd is 2.97 Å, the distance between the two Fe(III) ions in native Fd is 2.68 Å (Figure 1D and Table 3). A longer distance for the [2Ga-2S] cluster was also detected when analyzing the related small molecules, $[Et_4N]_2[Ga_2S_2(SPh)_4]$ and $[Et_4N]_2[Fe_2S_2(SPh)_4]$. In conclusion, the structural difference between the two metal clusters could be successfully accommodated in the cluster-binding loop.

DOI: 10.1021/acs.biochem.5b00601
Biochemistry 2015, 54, 6052−6061

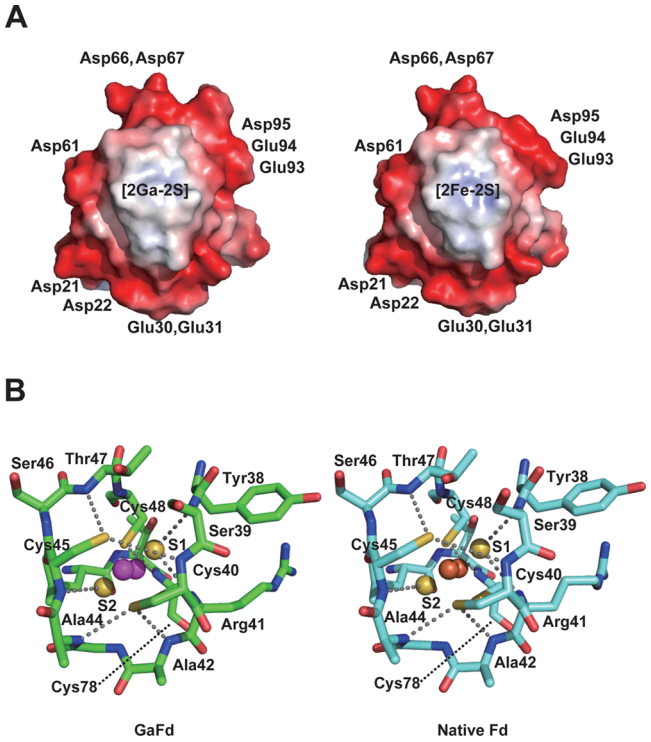

Figure 2. Structures surrounding the *Synechocystis* Ga-substituted Fd (GaFd) and native Fd. (A) Electrostatic potentials of GaFd (left) and native Fd (right) are mapped onto the molecular surfaces. Characteristic acidic patches are shown as residue names. For electrostatic surface potential, blue denotes positive and red negative. (B) Network of hydrogen bonds around the cluster of GaFd (left) and native Fd (right). Dotted lines are hydrogen bonds formed between S atoms in the cluster and the backbone amide groups listed in Table 2.

Hydrogen Bond Network of the [2Ga-2S] Cluster in *Synechocystis* GaFd. Plant-type Fd has a unique hydrogen bond network around the [2Fe-2S] cluster that is fundamentally conserved in the structures of oxidized Fd molecules.[5] Eight NH···S hydrogen bonds are formed between sulfur atoms in the cluster and the backbone amide hydrogen (Table 2 and Figure 2B). These hydrogen bonds are important for Fd's low redox potential. It was reported that after reduction of the native [2Fe-2S] cluster, another hydrogen bond is formed by the main chain amide hydrogen as result of flipping of the peptide bond between Cys46 and Ser47 (*Anabaena* sp. PCC 7119, hereafter named *Anabaena*).[36] This additional hydrogen bond between atom S2 of the cluster and the N atom of Ser47 was found only in the reduced state of Fd. It is important to know whether GaFd is an analogue of oxidized Fd or reduced Fd. In the vicinity of the [2Ga-2S] cluster of GaFd, the hydrogen bond network of oxidized native Fd was conserved and no hydrogen bond was formed between the S2 atom of the cluster and the N atom of Ser47. It is therefore apparent that GaFd was an analogue of oxidized Fd according to the hydrogen bond network around the cluster.

Table 2. NH···S Hydrogen Bond Distances between the Cluster and the Main Chain Amide Hydrogen[a]

	distance (Å)	
atoms involved in H-bonds	*Synechocystis* Fd	*Synechocystis* GaFd
N of Ser38···S1 of the cluster	3.24	3.28
N of Cys39···Sγ of Cys44	4.09	3.97
N of Arg40···S1 of the cluster	3.35	3.34
N of Ala41···Sγ of Cys39	3.34	3.24
N of Ala43···Sγ of Cys39	3.44	3.52
N of Cys44···S2 of the cluster	3.36	3.40
N of Thr46···Sγ of Cys44	3.25	3.33
N of Cys77···Sγ of Cys47	3.52	3.45

[a]Abbreviations: Fd, ferredoxin; GaFd, Ga-substituted ferredoxin.

Analysis of Binding Properties of GaFd and Native Fd from *Synechocystis* Using FNR_L Affinity Chromatography. The binding affinity of GaFd and native Fd for FNR was examined by an FNR_L-immobilized Sepharose resin. Both GaFd and native Fd bound to the FNR_L affinity column have been successfully eluted with a linear NaCl gradient. GaFd was eluted at 21.2 ± 0.70 mS/cm and native Fd at 21.1 ± 0.15 mS/cm (Figure S1 of the Supporting Information), i.e., the binding affinity between GaFd and native Fd is identical, suggesting that GaFd retains the nativelike binding/recognition properties to FNR_L. This finding is in good agreement with the results of X-ray crystallography described above and previous NMR analysis.[19]

Thermostability Assay of GaFd from *Synechocystis* and *T. elongatus*. The stability of a reconstituted protein is important for its structural analysis. Using a thermostability assay involving a CD spectropolarimeter (Jasco J-820, Jasco), the melting temperatures (T_m) of native Fds from *Synechocystis* and *T. elongatus* have been reported to be 71.2 ± 0.5 and 79.7 ± 2.8 °C, respectively, in contrast to GaFd samples with values of 58.8 ± 1.3 and 62.0 ± 5.4 °C, respectively. Native Fd of *T. elongatus* was more stable than Fd of *Synechocystis*, although their GaFd samples showed no significant differences. The decrease in thermostability upon replacement of the clusters was probably due to the subtle differences in the genometries of sulfurs and metals between the [2Fe-2S] and the [2Ga-2S] clusters (Table 3); however, this decrease was too small to be revealed by structural analysis.

Table 3. Distances between Two Atoms of the Cluster

	distance (Å)	
atoms[a]	*Synechocystis* Fd	*Synechocystis* GaFd
metal 1−metal 2	2.68	2.97
metal 1−S2	2.26	2.22
metal 2−S2	2.21	2.28
metal 1−S1	2.24	2.29
metal 2−S1	2.20	2.20
S1−S2	3.55	3.38

[a]The atom numbering corresponds to that of Figure 1B.

Determination of the Structure of *T. elongatus* Fd. The crystal structure of *T. elongatus* Fd was determined by the molecular replacement method and refined at 1.50 Å resolution (Table 1). Although the amino acid sequence of *T. elongatus* Fd is one residue longer than that of *Synechocystis* Fd and one residue shorter than that of Fd from *Anabaena*, their crystal structures resemble each other (*Anabaena* Fd was used for the X-ray analysis of the crystal structure of the Fd:FNR_S complex[18]). The rmsds for *Synechocystis* Fd (PDB entry 1OFF[9]) and *Anabaena* Fd (PDB entry 1CZP;[36] chain B was used for the calculation) were 0.5345 and 0.5284 Å for the C_α atoms, respectively; these data clearly indicated a similarity of the protein structures.

DOI: 10.1021/acs.biochem.5b00601
Biochemistry 2015, 54, 6052−6061

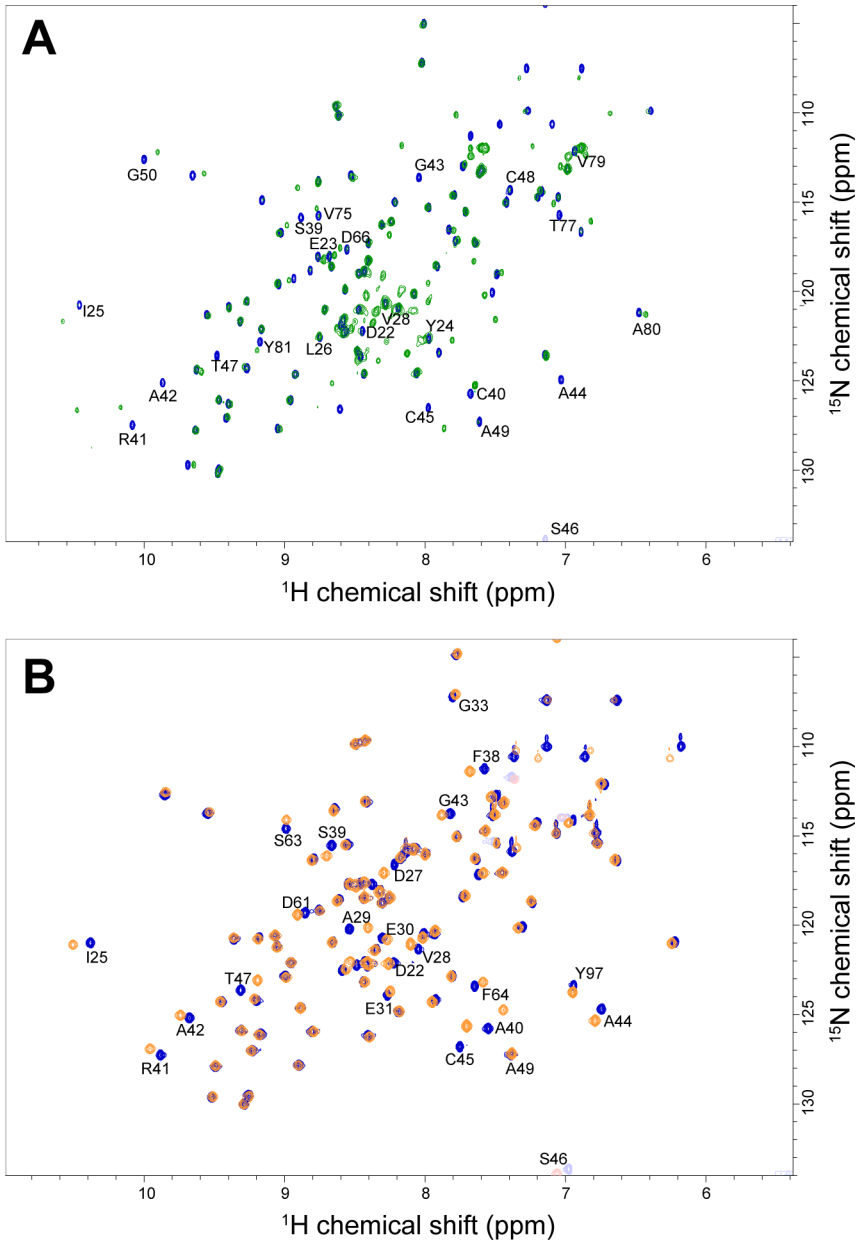

Figure 3. ^{1}H−^{15}N HSQC spectra of [^{15}N]GaFd. Overlay of the HSQC spectra in the absence (blue) and presence of PSI (A, green) or FNR$_S$ (B, orange). Broadening of NMR peaks is caused mainly by the exchange between bound and free forms, particularly when the exchange rate is close to the difference between the chemical shifts in the two states. Broadening, however, can also happen in residues remote from the interaction region. This may be due to a change in the dynamics in the remote region, induced by the interaction, or to transient formation of an encounter complex through electrostatic interaction, which is probable in a negatively charged hub protein, Fd. Chemical shifts may also be perturbed for the same reasons.

NMR Analysis of the Interaction Sites on GaFd. Application of NMR analysis for a huge membrane protein complex is a challenge in two respects: a lack of protein stability in the detergent micelle and the resultant large molecular size of the proteins. Under fast-exchange conditions such as those in the electron transfer complex, the transferred cross-saturation is one of the best methods for identifying the residues of protein ligands in the proximity of huge membrane proteins like PSI.[37] Nevertheless, the use of the stable oxidized Fd analogue, GaFd from the thermophilic *T. elongatus* without any electron transfer activity, also allowed us to measure perturbations of the NMR chemical shifts in the huge Fd:PSI complex [Figures 3A and 4A (top)]. Some peaks from the Fd:PSI complex disappeared because of the strong interaction with PSI [Figures 3A, 4A (top), and 4B (highlighted in blue)] or because of broadening of the related peaks due to association and dissociation. To visualize the spatial distribution of the interaction sites, we mapped the interface onto the crystal structure of *T. elongatus* Fd. The major interacting interface was classified into three major regions: region 1 including Asp22, Glu23, Tyr24, Ile25, and Val28; region 2 including Ser39, Cys40, Arg41, Ala42, Ser46, Thr47, and Gly50; and region 3 around Asp66, Gln69, Val75, Thr77, Val79, Ala80, and Tyr81 [Figures 3A, 4A (top), and 4B]. Regions 1 and 3 belong to the hydrophilic acidic patches that cover the surface of the Fd molecule. Region 2 comprises the cluster-binding loop that was invisible because of

DOI: 10.1021/acs.biochem.5b00601
Biochemistry 2015, 54, 6052−6061

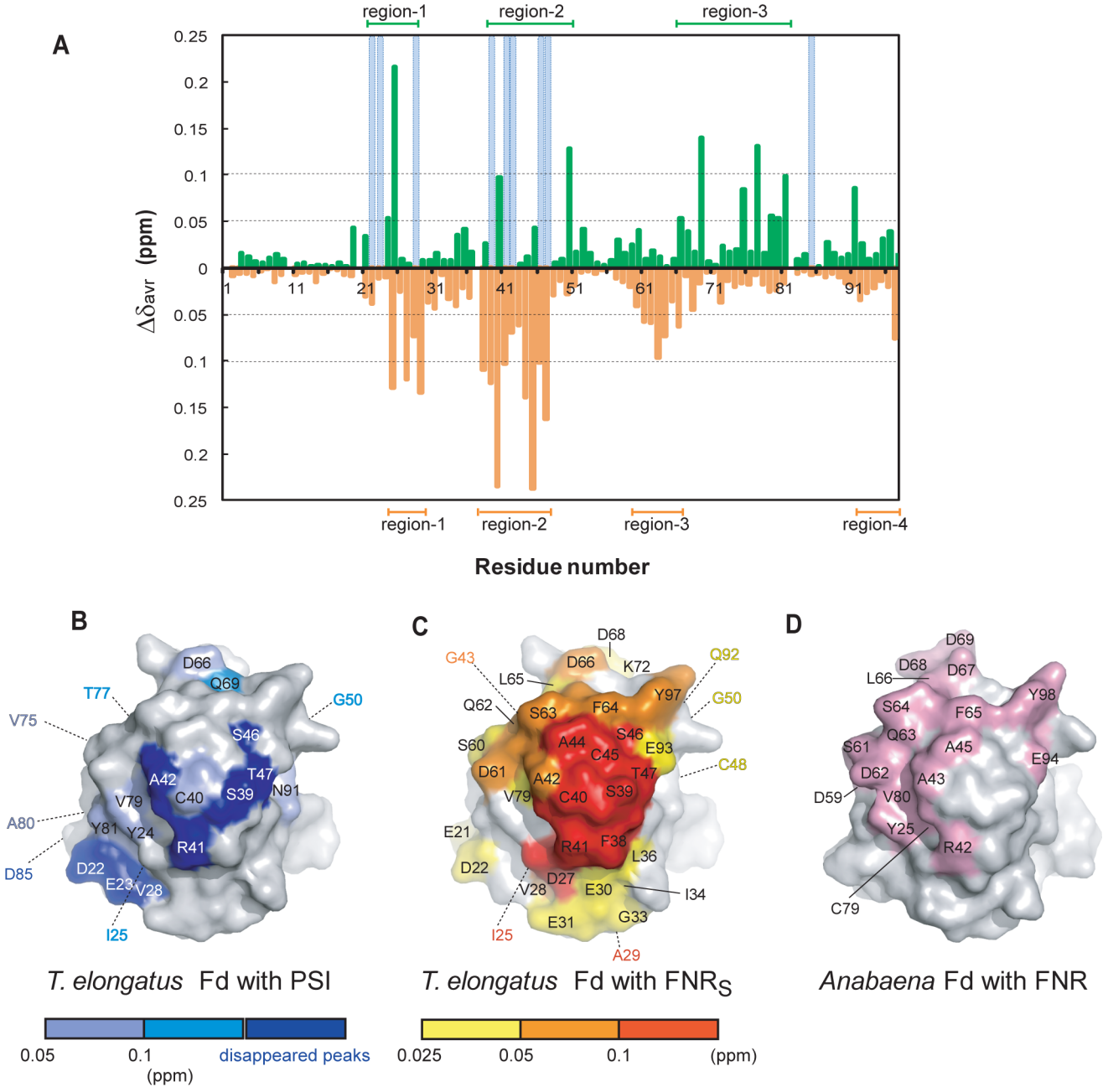

Figure 4. Comparison of chemical shift perturbations and mapping for Fd upon formation of the complex with PSI and FNR_S. (A) Chemical shift changes of [^{15}N]GaFd after formation of a complex with PSI (green) and FNR_S (orange). Interacting regions with PSI were classified as follows: region 1 (Asp22−Val28), region 2 (Ser39−Gly50), and region 3 (Asp66−Tyr81); regions with FNR_S were classified as follows: region 1 (Ile25−Ala29), region 2 (Phe38−Thr47), region 3 (Ser60−Asp66), and region 4 (Gln92−Tyr97). Blue columns represent residues whose peaks were broadened beyond detection upon formation of the complex with PSI. (B and C) Mapping of the chemical shift changes onto the three-dimensional structure of Fd for PSI (B) and FNR_S (C). Dotted lines indicate residues on the inside or on the backside. The residues are colored as follows: (B) 0.05−0.1 ppm (light blue), >0.1 ppm (blue), and "peaks disappeared" (dark blue) and (C) 0.025−0.05 ppm (yellow), 0.05−0.1 ppm (orange), and >0.1 ppm (red). (D) Surface representation of *Anabaena* Fd (PDB entry 1EWY[18,38]) colored in pink according to the distance (<5 Å) from FNR_S in the crystal structure. Distances have been calculated using the CONTACT program of the CCP4 software suite.[32]

the paramagnetic effect of Fe(III) in the original [2Fe-2S] cluster. In addition to the PSI data, we analyzed the chemical shifts in the Fd:FNR_S complex [Figures 3B and 4A (bottom)]. Although the map of the binding of [1Ga-0S]-type GaFd to spinach FNR had already been reported,[19] it was interesting to observe the effect of switching the cluster type to [2Ga-2S]. Mapping the FNR_S-binding sites onto the Fd structure showed an interaction pattern essentially identical to that of the [1Ga-0S]-type GaFd (Figure 4C). The loop region (Ser39−Ser46, *T. elongatus* numbering) covering the [2Ga-2S] cluster was located in the middle of the interacting interface even if we used the cyanobacterial FNR_S from *T. elongatus* instead of spinach FNR.

The fundamentally identical interaction patterns of GaFd with *T. elongatus* FNR_S and spinach FNR suggest the following model for the formation of the Fd:FNR_S complex in combination with the previously reported X-ray structure of Fd:FNR_S from *Anabaena*.[18,38] Conserved nonacidic Ser46 and Phe64 of *T. elongatus* Fd (Ser47 and Phe65 in *Anabaena* Fd and

DOI: 10.1021/acs.biochem.5b00601
Biochemistry 2015, 54, 6052−6061

Ser45 and Phe63 in *Synechocystis* Fd, respectively) are located near the metal center in the middle of the interacting interface, which is consistent with their involvement in FNR_S binding and mutational effects on the electron transfer activities.[39,40] The distribution of the surrounding acidic patches being used for FNR_S binding was slightly different from that in the previously published X-ray structure of the complex (Figure 4D, PDB entry 1EWY[18,38]). An additional patch named region 1 consisting of Glu30, Glu31, and Gly33 (*T. elongatus* numbering), which was prominent in the interaction with sulfite reductase,[21] was found to be involved in formation of the complex with FNR as already mentioned by Xu et al.[19]

In the NMR analysis of the Fd:FNR_S complex, we found that there are four major interacting regions of Fd [Figures 4A (bottom) and 4C]. Regions 1 and 2 are almost overlapped between the two complexes. In the X-ray structure of the Fd:FNR_S complex from *Anabaena* (PDB entry 1EWY[18,38]), region 2 is thought to be important for redox-dependent disassembly of the proteins. This is because the peptide bond between Cys46 and Ser47 (*Anabaena* numbering) should be flipped after the reduction of Fd. As the X-ray structure of the Fd:PSI complex is not yet available, we compared the results of the NMR analysis of GaFd with PSI and FNR_S. Apparently, the corresponding sites of Cys45 and Ser46 (*T. elongatus* numbering) are included in the interacting sites of the two complexes. Assuming that this redox-linked peptide flip occurs in general,[41] we propose here that the redox-linked conformational change in Fd might be a dissociation trigger also in case of the Fd:PSI complex. Results from this comparative NMR analysis accentuate the importance of the previously missing information with respect to the area around the cluster-binding loop that has been acquired only in GaFd instead of native Fd.

Within the Fd:FNR_S and Fd:PSI electron transfer complexes, the interacting region 2 is commonly located in the middle of the whole interface as discussed above. In contrast, the surrounding hydrophilic interaction regions 1, 3, and 4 are not identical in the two complexes. Region 1 was detected by only solution NMR analysis; region 3 did not exactly overlap between two complexes, and region 4 is FNR-specific. This flexible interaction pattern might be important for the fine-tuning of the interaction of a particular electron transfer complex and its transient characteristics of complex formation. As the crystal structure can show only one snapshot of the transient complex formation in general, analysis of the whole process of complex formation can be achieved only in combination with other, for instance, NMR-based, methods.

■ ASSOCIATED CONTENT

Supporting Information

The Supporting Information is available free of charge on the ACS Publications website at DOI: 10.1021/acs.biochem.5b00601.

Affinity chromatography of Ga-substituted Fd (GaFd) and native Fd on an FNR-immobilized resin (Figure S1) (PDF)

Accession Codes

The coordinates and structure factors for *Synechocystis* GaFd and *T. elongatus* Fd are available as PDB entries 5AUK and 5AUI, respectively. The resonance assignment for GaFd has been deposited in the Biological Magnetic Resonance Bank as accession number 11596.

■ AUTHOR INFORMATION

Corresponding Author

*Telephone: +81-6-6879-8604. Fax: +81-6-6879-8606. E-mail: gkurisu@protein.osaka-u.ac.jp.

Present Address

⊥N.M.: Institute for Molecular Science, National Institutes of Natural Sciences, 5-1 Higashiyama, Myodaiji, Okazaki 444-8787, Japan.

Author Contributions

R.M. and N.M. contributed equally to this work.

Funding

This work was supported in part by Grants-in-Aid for Scientific Research 11J05122 (to N.M.) and 13J03550 and 26870354 (H.K.-K.) and by the Funding Program for Next Generation World-Leading Researchers (GS016) from the Cabinet Office of Japan. M.M.N. and M.R. gratefully acknowledge the financial support by the European Union Seventh Framework Programme (FP7/2007-2013) under Grant Agreement 308518 (CyanoFactory).

Notes

The authors declare no competing financial interest.

■ ACKNOWLEDGMENTS

We are grateful to Mrs. Megumi Muraki-Taya for her contribution to the crystallization screening, to Professor Yuji Goto in the Institute for Protein Research, Osaka University (Osaka, Japan), for his help during CD measurement, and to Associate Professor Takuji Oyama in the Department of Biotechnology, Faculty of Life and Environmental Sciences, University of Yamanashi (Kofu, Japan), for his valuable support during the X-ray analysis.

■ ABBREVIATIONS

Fd, ferredoxin; GaFd, Ga-substituted ferredoxin; FNR, ferredoxin-$NADP^+$ reductase; PSI, Photosystem I; FTR, ferredoxin-thioredoxin reductase; NiR, nitrite reductase; CD, circular dichroism; T_m, melting temperature; HSQC, heteronuclear single-quantum coherence; rmsd, root-mean-square deviation.

■ REFERENCES

(1) Knaff, D. B. (1996) Ferredoxin and ferredoxin-dependent enzymes. In *Oxygenic Photosynthesis: The Light Reactions* (Ort, D. R., and Yocum, C. F., Eds.) pp 333−361, Kluwer, Dordrecht, The Netherlands.

(2) Akashi, T., Matsumura, T., Ideguchi, T., Iwakiri, K., Kawakatsu, T., Taniguchi, I., and Hase, T. (1999) Comparison of the Electrostatic Binding Sites on the Surface of Ferredoxin for Two Ferredoxin-dependent Enzymes, Ferredoxin-NADP+ Reductase and Sulfite Reductase. *J. Biol. Chem. 274*, 29399−29405.

(3) Kimata-Ariga, Y., Sakakibara, Y., Ikegami, T., and Hase, T. (2010) Electron transfer of site-specifically cross-linked complexes between ferredoxin and ferredoxin-NADP(+) reductase. *Biochemistry 49*, 10013−10023.

(4) Fukuyama, K., Hase, T., Matsumoto, S., Tsukihara, T., Katsube, Y., Tanaka, N., Kakudo, M., Wada, K., and Matsubara, H. (1980) Structure of S. platensis [2Fe-2S] ferredoxin and evolution of chloroplast-type ferredoxins. *Nature 286*, 522−524.

(5) Holden, H. M., Jacobson, B. L., Hurley, J. K., Tollin, G., Oh, B.-H., Skjeldal, L., Chae, Y. K., Cheng, H., Xia, B., and Markley, J. L. (1994) Structure-Function Studies of [2Fe-2S] Ferredoxins. *J. Bioenerg. Biomembr. 26*, 67−88.

DOI: 10.1021/acs.biochem.5b00601
Biochemistry 2015, 54, 6052−6061

(6) Binda, C., Coda, A., Aliverti, A., Zanetti, G., and Mattevi, A. (1998) Structure of the mutant E92K of [2Fe-2S] ferredoxin I from Spinacia oleracea at 1.7 A resolution. *Acta Crystallogr., Sect. D: Biol. Crystallogr. 54*, 1353−1358.
(7) Sakakibara, Y., Kimura, H., Iwamura, A., Saitoh, T., Ikegami, T., Kurisu, G., and Hase, T. (2012) A new structural insight into differential interaction of cyanobacterial and plant ferredoxins with nitrite reductase as revealed by NMR and X-ray crystallographic studies. *J. Biochem. 151*, 483−492.
(8) Kurisu, G., Nishiyama, D., Kusunoki, M., Fujikawa, S., Katoh, M., Hanke, G. T., Hase, T., and Teshima, K. (2004) A structural basis of Equisetum arvense ferredoxin isoform II producing an alternative electron transfer with ferredoxin-NADP+ reductase. *J. Biol. Chem. 280*, 2275−2281.
(9) Van den Heuvel, R. H. H., Svergun, D. I., Petoukhov, M. V., Coda, A., Curti, B., Ravasio, S., Vanoni, M. A., and Mattevi, A. (2003) The Active Conformation of Glutamate Synthase and its Binding to Ferredoxin. *J. Mol. Biol. 330*, 113−128.
(10) Karplus, P. A., Daniels, M. J., and Herriott, J. R. (1991) Atomic structure of ferredoxin-NADP+ reductase: prototype for a structurally novel flavoenzyme family. *Science 251*, 60−66.
(11) Serre, L., Vellieux, F. M. D., Medina, M., Gomez-Moreno, C., Fontecilla-Camps, J. C., and Frey, M. (1996) X-ray Structure of the Ferredoxin:NADP+ Reductase from the Cyanobacterium *Anabaena* PCC 7119 at 1.8 Å Resolution, and Crystallographic Studies of NADP + Binding at 2.25 Å Resolution. *J. Mol. Biol. 263*, 20−39.
(12) Dorowski, A., Hofmann, A., Steegborn, C., Boicu, M., and Huber, R. (2001) Crystal structure of paprika ferredoxin-NADP+ reductase. Implications for the electron transfer pathway. *J. Biol. Chem. 276*, 9253−9263.
(13) Twachtmann, M., Altmann, B., Muraki, N., Voss, I., Okutani, S., Kurisu, G., Hase, T., and Hanke, G. T. (2012) N-terminal Structure of Maize Ferredoxin:NADP+ Reductase Determines Recruitment into Different Thylakoid Membrane Complexes. *Plant Cell 24*, 2979−2991.
(14) Deng, Z., Aliverti, A., Zanetti, G., Arakaki, A. K., Ottado, J., Orellano, E. G., Calcaterra, N. B., Ceccarelli, E. A., Carrillo, N., and Karplus, P. A. (1999) A productive NADP+ binding mode of ferredoxin-NADP + reductase revealed by protein engineering and crystallographic studies. *Nat. Struct. Biol. 6*, 847−853.
(15) Dai, S., Friemann, R., Glauser, D. A., Bourquin, F., Manieri, W., Schurmann, P., and Eklund, H. (2007) Structural snapshots along the reaction pathway of ferredoxin-thioredoxin reductase. *Nature 448*, 92−96.
(16) Swamy, U., Wang, M., Tripathy, J. N., Kim, S. K., Hirasawa, M., Knaff, D. B., and Allen, J. P. (2005) Structure of spinach nitrite reductase: implications for multi-electron reactions by the iron-sulfur:siroheme cofactor. *Biochemistry 44*, 16054−16063.
(17) Kurisu, G., Kusunoki, M., Katoh, E., Yamazaki, T., Teshima, K., Onda, Y., Kimata-Ariga, Y., and Hase, T. (2001) Structure of the electron transfer complex between ferredoxin and ferredoxin-NADP-(+) reductase. *Nat. Struct. Biol. 8*, 117−121.
(18) Morales, R., Charon, M. H., Kachalova, G., Serre, L., Medina, M., Gomez-Moreno, C., and Frey, M. (2000) A redox-dependent interaction between two electron-transfer partners involved in photosynthesis. *EMBO Rep. 1*, 271−276.
(19) Xu, X., Scanu, S., Chung, J. S., Hirasawa, M., Knaff, D. B., and Ubbink, M. (2010) Structural and functional characterization of the ga-substituted ferredoxin from Synechocystis sp. PCC6803, a mimic of the native protein. *Biochemistry 49*, 7790−7797.
(20) Xu, X., Kim, S. K., Schurmann, P., Hirasawa, M., Tripathy, J. N., Smith, J., Knaff, D. B., and Ubbink, M. (2006) Ferredoxin/ferredoxin-thioredoxin reductase complex: Complete NMR mapping of the interaction site on ferredoxin by gallium substitution. *FEBS Lett. 580*, 6714−6720.
(21) Saitoh, T., Ikegami, T., Nakayama, M., Teshima, K., Akutsu, H., and Hase, T. (2006) NMR study of the electron transfer complex of plant ferredoxin and sulfite reductase: mapping the interaction sites of ferredoxin. *J. Biol. Chem. 281*, 10482−10488.
(22) Kazanis, S., Pochapsky, T. C., Barnhart, T. M., Penner-Hahn, J. E., Mirza, U. A., and Chait, B. T. (1995) Conversion of a Fe2S2 Ferredoxin into a Ga3+ Rubredoxin. *J. Am. Chem. Soc. 117*, 6625−6626.
(23) Vo, E., Wang, H. C., and Germanas, J. P. (1997) Preparation and characterization of [2Ga-2S] Anabaena 7120 ferredoxin, the first gallium-sulfur cluster-containing protein. *J. Am. Chem. Soc. 119*, 1934−1940.
(24) Thomas, J. C., Ughy, B., Lagoutte, B., and Ajlani, G. (2006) A second isoform of the ferredoxin:NADP oxidoreductase generated by an in-frame initiation of translation. *Proc. Natl. Acad. Sci. U. S. A. 103*, 18368−18373.
(25) Van Thor, J. J., Gruters, O. W. M., Matthijs, H. C. P., and Hellingwerf, K. J. (1999) Localization and function of ferredoxin:NADP+ reductase bound to the phycobilisomes of Synechocystis. *EMBO J. 18*, 4128−4136.
(26) Gomez-Lojero, C., Perez-Gomez, B., Shen, G., Schluchter, W. M., and Bryant, D. A. (2003) Interaction of ferredoxin:NADP+ oxidoreductase with phycobilisomes and phycobilisome substructures of the cyanobacterium Synechococcus sp. strain PCC 7002. *Biochemistry 42*, 13800−13811.
(27) Nakajima, M., Sakamoto, T., and Wada, K. (2002) The Complete Purification and Characterization of Three Forms of Ferredoxin-NADP+ Oxidoreductase from a Thermophilic Cyanobacterium Synechococcus elongatus. *Plant Cell Physiol. 43*, 484−493.
(28) Korn, A., Ajlani, G., Lagoutte, B., Gall, A., and Setif, P. (2009) Ferredoxin:NADP+ oxidoreductase association with phycocyanin modulates its properties. *J. Biol. Chem. 284*, 31789−31797.
(29) Prodöhl, A., Ambill, M., El-Mohsnawy, E., Lax, J., Nowaczyk, M., Oworah-Nkruma, R., Volkmer, T., Wenk, S.-O., and Rögner, M. (2004) Modular device for hydrogen production: Optimization of (individual) components, In *Biohydrogen III, Renewable Energy System by Biological Solar Energy Conversion* (Miyake, J., Igarashi, Y., and Rögner, M., Eds.) pp 171−179, Elsevier, Amsterdam.
(30) Kubota, H., Sakurai, I., Katayama, K., Mizusawa, N., Ohashi, S., Kobayashi, M., Zhang, P., Aro, E. M., and Wada, H. (2010) Purificatin and characterization of photosystem I complex from Synechocystis sp. PCC 6803 by expressing histidine-tagged subunits. *Biochim. Biophys. Acta, Bioenerg. 1797*, 98−105.
(31) Otwinowski, Z., and Minor, W. (1997) Processing of X-ray Diffraction Data Collected in Oscillation Mode. In *Methods in Enzymology* (Carter, C. W., and Sweet, R. M., Eds.) pp 307−326, Academic Press, New York.
(32) Collaborative Computational Project, Number 4 (1994) The CCP4 suite: programs for protein crystallography. *Acta Crystallogr., Sect. D: Biol. Crystallogr. 50*, 760−763.
(33) Emsley, P., and Cowtan, K. (2004) Coot: model-building tools for molecular graphics. *Acta Crystallogr., Sect. D: Biol. Crystallogr. 60*, 2126−2132.
(34) Maelia, L. E., and Koch, S. A. (1986) Gallium Analogues of Iron-Sulfide-Thiolate Compounds. Analysis of the Structural Parameters in Gallium(III) and Iron(III) Chalcogenide Compounds. *Inorg. Chem. 25*, 1896−1904.
(35) Lovell, S. C., Davis, I. W., Arendall, W. B., 3rd, de Bakker, P. I., Word, J. M., Prisant, M. G., Richardson, J. S., and Richardson, D. C. (2003) Structure validation by Calpha geometry: phi,psi and Cbeta deviation. *Proteins: Struct., Funct., Genet. 50*, 437−450.
(36) Morales, R., Charon, M. H., Hudry-Clergeon, G., Petillot, Y., Norager, S., Medina, M., and Frey, M. (1999) Refined X-ray structures of the oxidized, at 1.3 A, and reduced, at 1.17 A, [2Fe-2S] ferredoxin from the cyanobacterium Anabaena PCC7119 show redox-linked conformational changes. *Biochemistry 38*, 15764−15773.
(37) Ueda, T., Nomoto, N., Koga, M., Ogasa, H., Ogawa, Y., Matsumoto, M., Stampoulis, P., Sode, K., Terasawa, H., and Shimada, I. (2012) Structural basis of efficient electron transport between photosynthetic membrane proteins and plastocyanin in Spinach revealed using nuclear magnetic resonance. *Plant Cell 24*, 4173−4186.
(38) Hurley, J. K., Salamon, Z., Meyer, T. E., Fitch, J. C., Cusanovich, M. A., Markley, J. L., Cheng, H., Xia, B., Chae, Y. K., Medina, M.,

DOI: 10.1021/acs.biochem.5b00601
Biochemistry 2015, 54, 6052−6061

Gomez-Mereno, C., and tollin, G. (1993) Amino acid residues in Anabaena ferredoxin crucial to interaction with ferredoxin-NADP+ reductase: site-directed mutagenesis and laser flash photolysis. *Biochemistry 32*, 9346−9354.
(39) Hurley, J. K., Weber-Main, A. M., Stankovich, M. T., Benning, M. M., Thoden, J. B., Vanhooke, J. L., Holden, H. M., Chae, Y. K., Xia, B., Cheng, H., Markley, J. L., Martine-Júlvez, M., Gómez-Moreno, C., Schmeits, J. L., and Tollin, G. (1997) Structure-function relationships in Anabaena ferredoxin: correlations between X-ray crystal structures, reduction potentials, and rate constants of electron transfer to ferredoxin: NADP+ reductase for site-specific ferredoxin mutants. *Biochemistry 36*, 11100−11117.
(40) Morales, R., Kachalova, G., Vellieux, F., Charon, M. H., and Frey, M. (2000) Crystallographic studies of the interaction between the ferredoxin-$NADP^+$ reductase and ferredoxin from the cyabacterium *Anabaena*: looking for the elusive ferredoxin molecule. *Acta Crystallogr., Sect. D: Biol. Crystallogr. D56*, 1408−1412.
(41) Morales, R., Frey, M., and Mouesca, J. M. (2002) An approach based on quantum chemistry calculations and structural analysis of a [2Fe-2S*] ferredoxin that reveal a redox-linked switch in the electron-transfer process to the Fd-$NADP^+$ reductase. *J. Am. Chem. Soc. 124*, 6714−6722.
(42) *The PyMOL Molecular Graphics System*, version 1.3r1 (2010) Schrodinger, LLC, Portland, OR.

DOI: 10.1021/acs.biochem.5b00601
Biochemistry 2015, 54, 6052−6061